Activation and integration of bilateral GABA-mediated synaptic inputs in neonatal rat sympathetic preganglionic neurones *in vitro*

Andrew D. Whyment[1], Jennifer M. M. Wilson[2], Leo P. Renaud[2] and David Spanswick[1]

[1] *Department of Biological Sciences, University of Warwick, Coventry CV4 7AL, UK*
[2] *Neurosciences Program, Ottawa Health Research Institute and University of Ottawa, Ottawa, Ontario, Canada, K1Y 4E9*

The role of GABA receptors in synaptic transmission to neonatal rat sympathetic preganglionic neurones (SPNs) was investigated utilizing whole-cell patch clamp recording techniques in longitudinal and transverse spinal cord slice preparations. In the presence of glutamate receptor antagonists (NBQX, 5 μM and D-APV, 10 μM), electrical stimulation of the ipsilateral or contralateral lateral funiculi (iLF and cLF, respectively) revealed monosynaptic inhibitory postsynaptic potentials (IPSPs) in 75% and 65% of SPNs, respectively. IPSPs were sensitive to bicuculline (10 μM) in all neurones tested and reversed polarity around -55 mV, the latter indicating mediation via chloride conductances. In three neurones IPSPs evoked by stimulation of the iLF ($n = 1$) or cLF ($n = 2$) were partly sensitive to strychnine (2 μM). The expression of postsynaptic GABA$_A$ and GABA$_B$ receptors were confirmed by the sensitivity of SPNs to agonists, GABA (2 mM), muscimol (10–100 μM) or baclofen (10–100 μM), in the presence of TTX, each of which produced membrane hyperpolarization in all SPNs tested. Muscimol-induced responses were sensitive to bicuculline (1–10 μM) and SR95531 (10 μM) and baclofen-induced responses were sensitive to 2-hydroxy-saclofen (100–200 μM) and CGP55845 (200 nM). The GABA$_C$ receptor agonist CACA (200 μM) was without significant effect on SPNs. These results suggest that SPNs possess postsynaptic GABA$_A$ and GABA$_B$ receptors and that subsets of SPNs receive bilateral GABAergic inputs which activate GABA$_A$ receptors, coupled to a chloride conductance. At resting or holding potentials close to threshold either single or bursts (10–100 Hz) of IPSPs gave rise to a rebound excitation and action potential firing at the termination of the burst. This effect was mimicked by injection of small (10–20 pA) rectangular-wave current pulses, which revealed a time-dependent, Cs$^+$-sensitive inward rectification and rebound excitation at the termination of the response to current injection. Synaptic activation of a rebound excitation mediated by a time-dependent inward rectification expressed intrinsically by SPNs may provide a novel mechanism enabling SPNs to be entrained to rhythms driven from the brainstem or higher centres.

Sympathetic preganglionic neurones (SPNs), located predominantly within the intermediolateral cell column (IML) of the thoracolumbar spinal cord, receive extensive descending inputs from supraspinal sites and visceral and somatic afferent pathways at the level of the spinal cord (Coote, 1988). They function to integrate and co-ordinate these inputs to formulate the final central sympathetic motor command to the viscera.

Considerable evidence exists supporting a role for GABA as a neurotransmitter to SPNs including electrophysiological data (Backman & Henry, 1983; Inokuchi *et al.* 1992; Dun *et al.* 1993; Krupp & Feltz, 1993; Deuchars *et al.* 1997), electron-microscopic data (Bogan *et al.* 1989; Cabot *et al.* 1995; Llewellyn-Smith *et al.* 1995) and histochemical data (Bacon & Smith, 1988; Chiba & Semba, 1991; Llewellyn-Smith *et al.* 1995, 1997, 1998, 2002). Indeed, it has been proposed that GABAergic boutons comprise up to half of the total innervation of SPNs (Llewellyn-Smith *et al.* 1995, 1998). Despite the extensive literature supporting a role for GABA as a

neurotransmitter to SPNs, relatively little is known of the functional roles of GABA receptors in SPNs, the receptors mediating synaptic transmission and how SPNs integrate this information to formulate output responses. Here we demonstrate the expression of functional postsynaptic $GABA_A$ and $GABA_B$ receptors and a role for GABA in the bilateral regulation of SPNs. We further demonstrate that GABA-mediated synaptic inputs can lead to activation of intrinsic conductances conducive to generation of burst firing patterns of activity. Such a mechanism could be important in entrainment of SPNs to sympathetic rhythms. Part of this work has been previously published in abstract form (Wilson & Spanswick, 1998; Whyment *et al.* 2000).

Methods

Slice preparation

Electrophysiological recordings were made from transverse and longitudinal thoracolumbar spinal cord slices as previously described (Logan *et al.* 1996). Briefly, Sprague–Dawley or Wistar Kyoto rats, aged 7–16 days (either sex), were terminally anaesthetized using 4% Enflurane in O_2 (Abbott laboratories, Queensborough, Kent, UK) and decapitated, the spinal cord was removed and transverse or longitudinal sections were cut into 300–450 μm thick slices using either a Vibratome (Technical Products International Inc., St Louis, MO, USA) or Leica VT1000S (Leica Microsystems UK, Milton Keynes, UK). Slices were maintained in artificial cerebrospinal fluid (aCSF) at room temperature for 1 h after slicing before transferring to a recording chamber. For recording, individual slices were held between two grids in a custom-built chamber continuously perfused with aCSF at a rate of 4–10 ml·min^{-1}, illuminated from below and viewed under a dissection microscope. The aCSF was of the following composition (mM): NaCl, 127; KCl, 1.9; KH_2PO_4, 1.2; $CaCl_2$, 2.4; $MgCl_2$, 1.3; $NaHCO_3$, 26; D-glucose, 10; equilibrated with 95% O_2/5% CO_2.

Electrophysiological recordings

Whole cell recordings were performed at room temperature from neurones in the IML with an Axopatch 1D amplifier (Axon Instruments, Union City, CA, USA), using methods described in detail previously (Logan *et al.* 1996; Spanswick *et al.* 1998). Patch pipettes were pulled from thin-walled borosilicate glass (GC150-TF10, Clarke Electromedical, Pangbourne, Berkshire, UK) and had resistances of between 3 and 8 MΩ when filled with intracellular solution of the following composition (mM):

potassium gluconate, 130; KCl, 10; $MgCl_2$, 2; $CaCl_2$, 1; EGTA-Na, 1; Hepes, 10; Na_2ATP, 2; Lucifer yellow, 2 (or biocytin, 5); pH adjusted to 7.4 with KOH, osmolarity adjusted to 310 mosmol l^{-1} with sucrose. Series resistance compensation of approximately 70–80% was applied for whole-cell voltage clamp experiments. Correction of the liquid junctional potential was applied to whole-cell recordings and access resistance ranged between 5 and 25 MΩ. Neuronal input resistances were measured by injecting small rectangular-wave hyperpolarizing current pulses (10–50 pA) and measuring the amplitude of resulting electrotonic potentials. Recordings were monitored on an oscilloscope (Gould 1602, Gould Instrument Systems), displayed on a chart recorder (Gould, Easygraf TA240) and stored on either VHS (Sony, SLV-E230, signals being digitized at 2 kHz (Sony, PCM-701ES)), or digital audio tapes (Biologic, DTR-1205) for later off-line analysis. In addition, data were filtered at 2–5 kHz (1 kHz for voltage clamp data), digitized at 2–10 kHz (Digidata 1200A, Axon Instruments) and stored on a PC running pCLAMP 8.2 data acquisition software. Analysis of electrophysiological data was carried out using Clampfit 8.2 software (Axon Instruments). SPNs were identified as previously described (Logan *et al.* 1996; Spanswick *et al.* 1998). Briefly, SPNs were identified according to their characteristic morphology revealed postrecording by the presence of biocytin or Lucifer yellow introduced from the recording electrode, location in the lateral horn and characteristic electrophysiological properties.

Bipolar concentric stimulating electrodes (Clark Electromedical, Pangbourne, Berkshire, UK) were used to stimulate (1–10 V, 0.2 ms, 0.03–0.1 Hz, unless otherwise stated) either the ipsi- or contra-lateral lateral funiculi (iLF and cLF, respectively). In longitudinal slices, a diagonal cut was made at the caudal end of slices to ensure correct orientation of the slice in the recording chamber and positioning of stimulating electrodes rostral to the recording electrode. The latency of synaptic responses was measured relative to the onset of the stimulus artefact.

Statistical analyses

Statistical analysis was performed using Excel 2002 (Microsoft) with all values given as means ± S.E.M. Statistical significance was determined using Student's two-tailed *t* tests, paired or unpaired as appropriate. $P < 0.05$ was taken to indicate statistical significance.

Drugs

The following drugs were used: baclofen (10–100 μM), bicuculline methiodide (1–10 μM), caesium chloride

(CsCl$_2$, 1–10 mM), γ-aminobutyric acid (GABA, 2 mM), idazoxan hydrochloride (200 nM), muscimol (10–100 μM), 6-nitro-7-sulfamoylbenzo(f)quinoxaline-2,3-dione (NBQX, 5 μM), strychnine hydrochloride (2 μM) and yohimbine hydrochloride (1 μM) (all from Sigma); *cis*-4-aminocrotonic acid (CACA, 200 μM), D(−)2-amino-5-phosphonopentanoic acid (D-APV, 10 μM), (RS)-3-amino-2-(4-chlorophenyl)-2-hydroxypropyl-sulphonic acid (2-hydroxysaclofen, 100–200 μM), 2-(3-carboxypropyl)-3-amino-6-(p-methoxy-phenyl)pyridazinium bromide (SR95531, 10 μM) ((2S)-3-[[(1S)-1-(3,4-dichlorophenyl-0-ethyl] amino-2-hydroxy-propyl](phenylmethyl) phosphinic acid (CGP 55845, 200 nM), and 4-(N-ethyl-N-phenylamino)-1,2-dimethyl-6-(methylamino) pyrimidium chloride (ZD7288, 10 μM) (all from Tocris Cookson, Bristol, UK) and tetrodotoxin (TTX, 500 nM, from Alomone Laboratories, Israel).

CGP55845 and NBQX were prepared as a stock solution using 100% DMSO (Sigma) and diluted to the required concentration in aCSF immediately prior to use, resulting in a maximal DMSO concentration of < 0.1%. All other drugs were prepared as stock solutions in distilled water and diluted to the required concentration in aCSF immediately prior to use. The drugs were administered to the slice by perfusion from 50 ml syringes arranged in line with the main aCSF reservoir by a series of three-way valves. The agonist final concentrations reported represent the concentrations within the perfusion system and take no account of dilution within the recording chamber. Antagonists were applied for at least 10 min prior to the addition of agonists to ensure complete equilibration within the recording chamber.

Results

Whole-cell recordings from 176 neurones, identified as SPNs on the basis of their characteristic morphology and electrophysiological properties, were included in this study. Morphology was revealed with either Lucifer
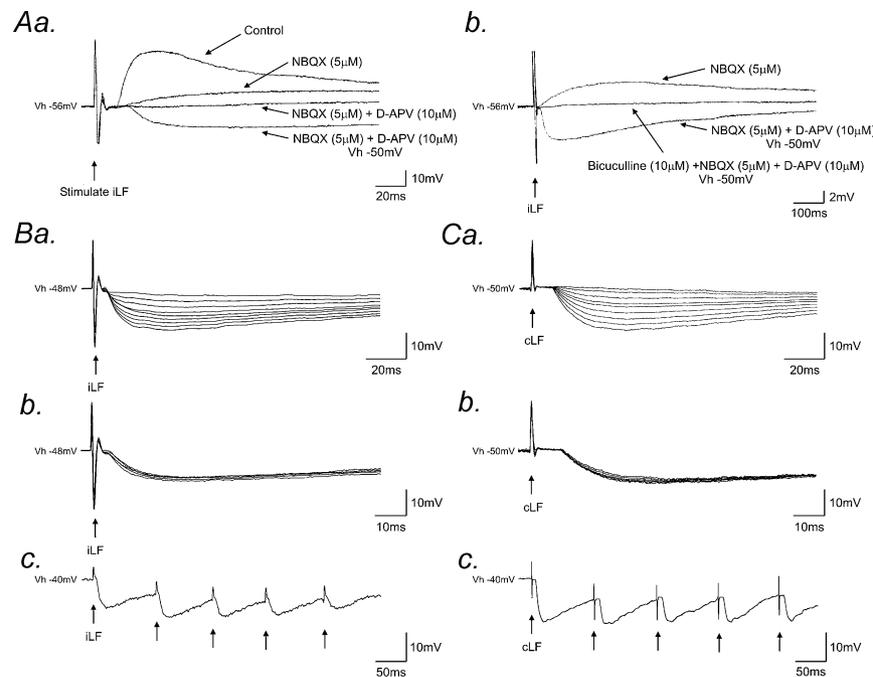
Figure 1. Exposure and properties of IPSPs evoked by stimulation of the lateral funiculi
Aa, block of fast excitatory synaptic transmission reveals underlying IPSPs. Superimposed samples of whole-cell current-clamp recordings from an SPN showing a fast (f)EPSP evoked by stimulation of the iLF. The fEPSP (Control) was reduced in the presence of NBQX (5 μM) and completely abolished by subsequent addition of D-APV (10 μM). Subsequent membrane depolarization (V_h − 50 mV) revealed a fIPSP. *Ab*, records from the same neurone as in *Aa*, shown on a longer time base. The GABA$_A$ receptor antagonist, bicuculline (V_h − 50 mV) completely blocked the fIPSP. All traces are the average of 16 consecutive responses. *Ba*, IPSPs (V_h − 48 mV) showed a graded response to increasing stimulus intensity of the iLF. Nine superimposed records are shown, each the average of six consecutive responses. *Bb*, five superimposed IPSPs (V_h − 48 mV) evoked by stimulation of the iLF showing constant rise time and latency and, *Bc*, no failures upon repetitive high-frequency stimulation (V_h − 40 mV). *C*, responses from the same neurone as shown in *B* to stimulation of the cLF. Note the relatively long latency compared to IPSPs evoked by stimulation of the iLF.

yellow or biocytin, revealing somata located within the lateral horn, medially projecting dendrites and an axon that coursed towards the ventral horn in transverse slices (see Spanswick *et al.* 1998). The characteristic electrophysiological profile of SPNs included a relatively long duration (5–10 ms) action potential with a distinct shoulder in the repolarizing phase, large amplitude (18–30 mV) afterhyperpolarization (AHP) and transient outward rectification observed as a delay in the return to rest of the voltage response following a series of hyperpolarizing current pulses (Spanswick *et al.* 1998). SPNs included in this study had a mean resting membrane potential of -53.9 ± 4.9 mV and a mean resting input resistance of 568 ± 77 MΩ.

Isolation of GABA-mediated synaptic inputs to SPNs

Electrical stimulation (0.03–0.1 Hz) of either the iLF or cLF evoked fast excitatory postsynaptic potentials (EPSPs) or excitatory postsynaptic currents (EPSCs) in all SPNs tested ($n = 36$). Application of the non-NMDA receptor antagonist NBQX (5 μM) and the NMDA receptor antagonist D-APV (10 μM) reversibly blocked these fast EPSPs in all neurones and unmasked fast IPSPs in 27/36 (75%) and 17/26 (65%) of SPNs following stimulation of the iLF and cLF, respectively (Fig. 1*Aa*). IPSPs had mean latency, 10–90% rise time and half-decay times of 2.4 ± 0.3, 8.1 ± 1.9 and 47 ± 5 ms, respectively (means $\pm$ s.e.m.),

following stimulation of the iLF (data from 27 neurones, values calculated from averages of 16 consecutively evoked responses for each neurone) and 7.8 ± 1.7, 10.1 ± 1.9 and 56 ± 4 ms, respectively, following stimulation of the cLF (data from 17 neurones, values calculated from averages of 16 consecutively evoked responses for each neurone) at holding or resting potentials between -35 and -50 mV. IPSPs showed graded responses to increasing stimulus intensity (Fig. 1*Ba* for iLF; Fig. 1*Ca* for cLF.), constant rise time (Fig. 1*Bb* and *Cb*) and no failures upon repetitive stimulation (10–100 Hz, Fig. 1*Bc* and *Cc*) suggesting a monosynaptic origin.

In some SPNs, slow noradrenergic IPSPs (Yoshimura *et al.* 1987*a*) were evoked upon stimulation of the LF (data not shown). To eliminate contamination of GABA-mediated IPSPs with concurrent noradrenergic synaptic responses, the $\alpha2$ receptor antagonists idazoxan (200 nM) and/or yohimbine (1 μM) were routinely included in the applied drug solutions.

Application of the GABA$_A$ receptor antagonists bicuculline (1–10 μM, $n = 27$; Figs 1*Ab* and 2) and SR95531 (10 μM, $n = 4$; data not shown) reversibly abolished IPSPs in a concentration-dependent manner. The threshold for bicuculline-induced complete inhibition of IPSPs or IPSCs was 5 μM (Fig. 2*A*). In addition, in three neurones, IPSCs evoked by stimulation of the iLF ($n = 1$) or cLF ($n = 2$) were partially suppressed upon application of the glycine receptor antagonist, strychnine (2–5 μM) and
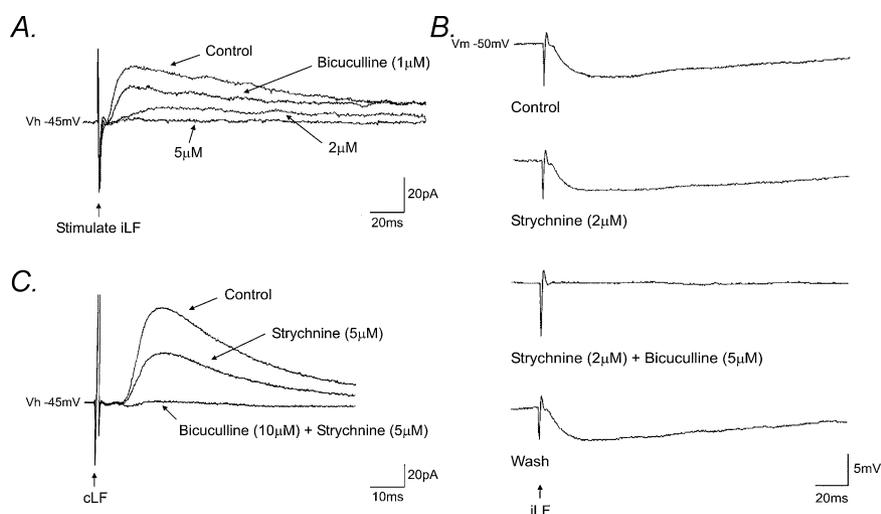
Figure 2. IPSPs evoked by stimulation of the lateral funiculi were mediated by GABA
A, superimposed voltage-clamp records of IPSCs evoked by stimulation of the iLF in the presence of NBQX and D-APV. IPSCs were progressively reduced in the presence of increasing concentrations of bicuculline ($V_h - 45$ mV). *B*, corresponding whole-cell current-clamp recording ($V_m - 50$ mV) showing IPSPs which were insensitive to strychnine, but completely and reversibly abolished by bicuculline. *C*, stimulation of the cLF evoked IPSCs which were reduced in the presence of strychnine and completely abolished by subsequent addition of bicuculline ($V_h - 45$ mV). Each record is the average of 8 consecutive responses.

subsequently abolished by bicuculline (Fig. 2*B* and *C*). IPSPs (Fig. 3*Aa*) and IPSCs (Fig. 3*Ba*) increased in peak amplitude upon membrane depolarization and decreased and reversed polarity upon membrane hyperpolarization to potentials more negative than around −55 mV. The mean reversal potential for IPSPs and IPSCs were −57 ± 2 mV (*n* = 6) and −56 ± 2 mV (*n* = 4) for the iLF (Fig. 3*Ab*) and the cLF (Fig. 3*Bb*), respectively, close to the reversal potential for chloride ions under our recording conditions.

To further clarify the origins of these fast IPSPs, we investigated their properties in a longitudinal slice preparation in the presence of glutamate (NBQX and D-APV) and glycine receptor (strychnine) antagonists. Stimulation of the iLF, rostral to the recording site, evoked IPSPs and IPSCs with mean latency, 10–90% rise time and half-decay time of 5.5 ± 2.1, 7.9 ± 1.2 and 45 ± 11 ms, respectively (*n* = 7). The corresponding values for IPSPs evoked by stimulation of cLF were 12.1 ± 2.8, 8.4 ± 1.2 and 49 ± 10 ms, respectively (*n* = 7). IPSPs evoked under these recording conditions were also monosynaptic in origin indicated by their constant latency, rise time and lack of failures upon repetitive stimulation. Analysis of the onset latency of IPSPs, measured from the onset of the stimulus artefact, upon repetitive stimulation (10 Hz) varied by 136 ± 11 μs. Monosynaptic IPSPs in longitudinal slices

were evoked in response to stimulation of the iLF (*n* = 3) and cLF (*n* = 2) up to several segments caudal to the recording site. Bath application of bicuculline (10 μM) completely and reversibly blocked all IPSPs and IPSCs recorded in response to stimulation of the iLF (*n* = 5) and cLF (*n* = 5). In all experiments in which GABA-mediated synaptic responses were isolated, we failed to identify any slow $GABA_B$ receptor-mediated component.

The effects of GABA receptor agonists on SPN

To further clarify the properties of postsynaptic GABA receptors on SPNs, the effects of GABA receptor agonists were investigated on 49 neurones. GABA (2 mM, *n* = 6), the $GABA_A$ receptor agonist muscimol (10–100 μM, *n* = 24), the $GABA_B$ receptor agonist baclofen (10–100 μM, *n* = 15) or the $GABA_C$ receptor agonist CACA (200 μM, *n* = 4) was bath applied to the slice by superfusion for 10–120 s. Bath application of GABA induced membrane hyperpolarization in all SPNs tested. The response was characterized by hyperpolarization of the membrane from a mean resting or holding potential of −45.3 ± 1.9 mV to −52.0 ± 2.0 mV, a mean peak membrane hyperpolarization of 6.7 ± 1.6 mV (Fig. 4*B*). GABA-induced membrane hyperpolarization was associated with
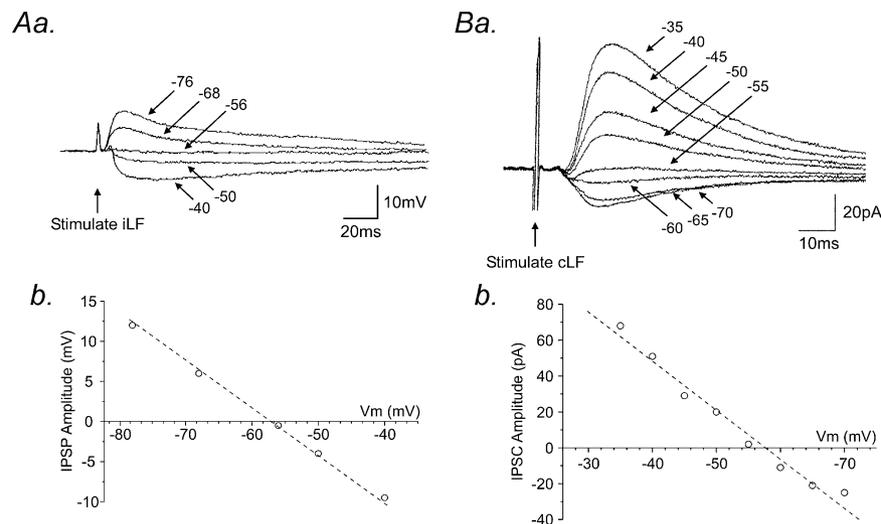

Figure 3. GABA receptor-mediated IPSPs and IPSCs are mediated via a chloride conductance
Aa, superimposed samples of a continuous whole-cell current-clamp recording showing the effects of changes in membrane potential on IPSPs evoked by stimulation of the iLF. Progressive membrane hyperpolarization of the SPN from −40 to −76 mV initially reduced the amplitude and subsequently reversed polarity of the IPSPs at potentials more negative than around −55 mV, close to the reversal potential for chloride ions under our recording conditions. *Ab*, plot of data shown in *a*. *Ba*, same neurone as *A* showing superimposed whole-cell voltage-clamp recordings of the effects of changes in holding potential on the amplitude of the IPSC evoked by stimulation of the cLF. IPSCs were progressively reduced in amplitude and reversed polarity with increasingly negative holding potentials. *Bb*, plot of data shown in *a*. Note the reversal potential close to the chloride reversal potential of −55 mV. All records are the average of eight consecutive responses recorded in the presence of NBQX (5 μM) and D-APV (10 μM).

a concurrent reduction in neuronal input resistance from a mean of 550 ± 50 MΩ at rest to 250 ± 42 MΩ in the presence of GABA, amounting to a $54.6 \pm 3.9\%$ decrease (Fig. 4B). Muscimol application produced membrane hyperpolarization in 17 cells from a mean resting or holding potential of -45.9 ± 4.9 mV to -51.9 ± 3.6 mV, a mean hyperpolarization of 6.0 ± 0.6 mV at the peak of response (Fig. 4Aa and b). A membrane depolarization was observed in seven SPNs, at resting potentials more negative than the chloride reversal potential under our recording conditions, from a mean resting potential of -60.3 ± 2.7 mV to -52.7 ± 1.9 mV, a mean depolarization of $7.6 \pm$

1.2 mV (Fig. 4Ab). A concurrent decrease in neuronal input resistance was observed in all cells tested, from a mean of 556 ± 28 MΩ at rest to 283 ± 27 MΩ in the presence of muscimol, a $49.6 \pm 3.2\%$ decrease and from 584 ± 48 MΩ to 291 ± 36 MΩ, a $48.2 \pm 6.9\%$ decrease for the hyperpolarizing and depolarizing response, respectively (Fig. 4B). CACA had no statistically significant effect on either membrane potential or input resistance ($n = 4$; Fig. 4B).
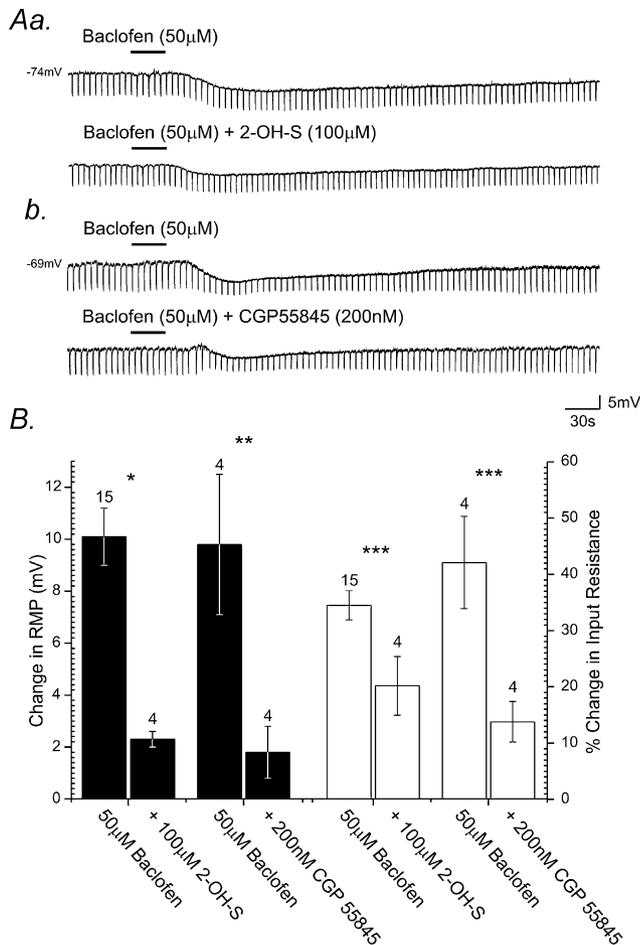
Application of baclofen induced membrane hyperpolarization in all cells tested, from a mean resting value of -60.0 ± 2.5 mV to -70.1 ± 3.6 mV,
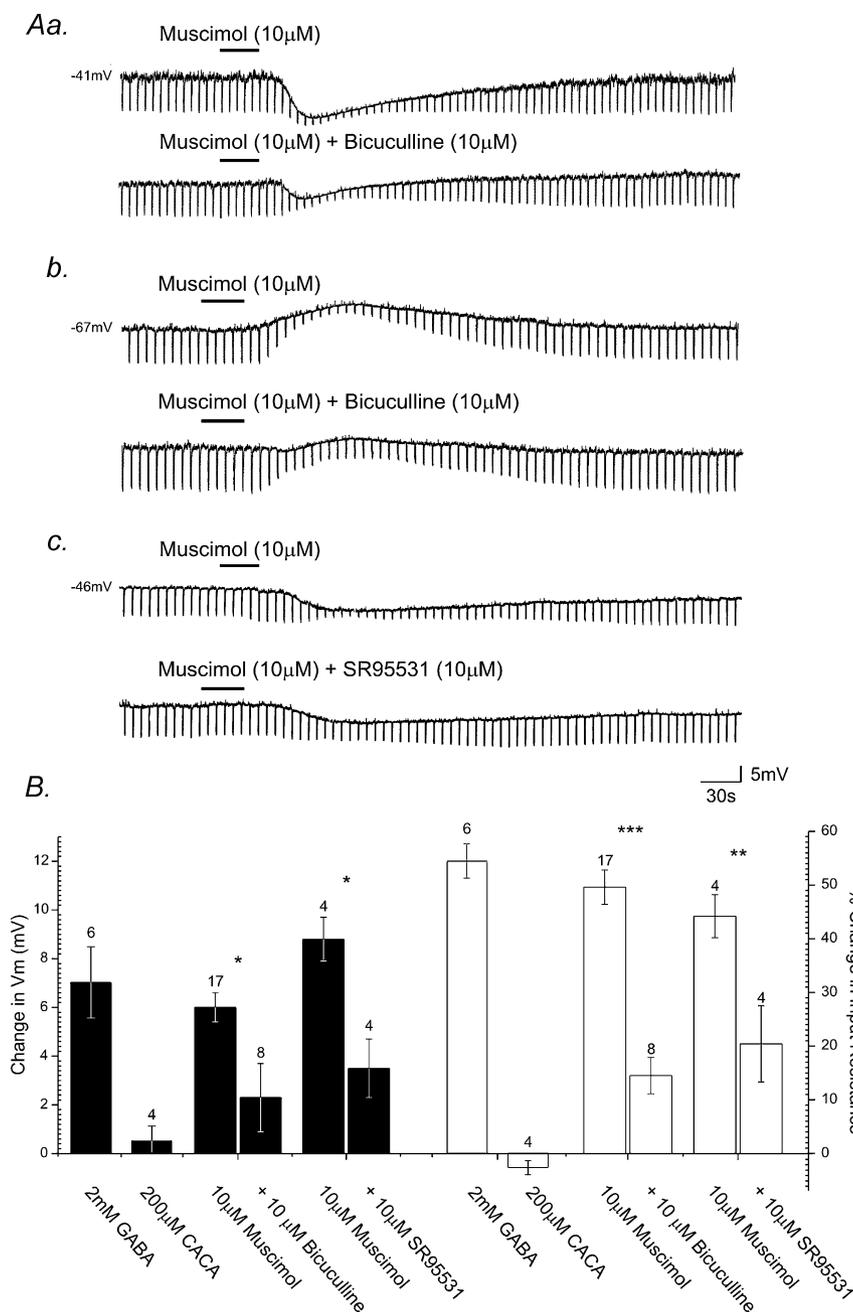
Figure 4. SPNs express postsynaptic GABA$_A$ receptors
Aa, samples of a continuous whole-cell current-clamp recording from an SPN showing muscimol-induced hyperpolarization and concomitant decrease in neuronal input resistance, indicated by the fall in amplitude of electrotonic potentials (downward deflections of the records) evoked in response to hyperpolarizing rectangular wave current pulses (not shown). Subsequent application of bicuculline reduced the response to muscimol. *Ab*, bath application of muscimol to another SPN induced membrane depolarization and an associated decrease in neuronal input resistance. Application of bicuculline reversibly reduced the magnitude of this response to muscimol. *Ac*, in another SPN muscimol-induced hyperpolarization was reduced in the presence of SR95531. *B*, summary histogram illustrating the pharmacological profile of ionotropic GABA receptor-mediated responses evoked in SPNs. The peak membrane potential responses (filled columns) and changes in neuronal input resistance (open columns) induced by GABA receptor agonists and the effects of antagonists on agonist-induced responses are shown. Error bars represent s.e.m. Numbers above individual bars indicate number of cells tested (*n*). (*$P < 0.01$, **$P < 0.03$, ***$P < 0.001$.)

a mean peak membrane hyperpolarization of 10.1 ± 1.1 mV (Fig. 5Aa, Ab and B). This hyperpolarization was again associated with a pronounced decrease in neuronal input resistance from a resting value of 398 ± 90 MΩ to 235 ± 82 MΩ, amounting to a $34.4 \pm 2.6\%$ decrease (Fig. 5B). All responses persisted in the presence of TTX (500 nM) and were at least partially reversible upon wash.

Figure 5. SPNs express postsynaptic GABA$_B$ receptors
Aa, samples of a continuous whole-cell current-clamp recording from an SPN showing bath application of baclofen, induces membrane hyperpolarization associated with a decrease in neuronal input resistance. Subsequent application of 2-hydroxy-saclofen (2-OH-S) reduced the membrane response induced by baclofen. *Ab*, bath application of baclofen to another SPN induced membrane hyperpolarization corresponding with a decrease in neuronal input resistance. Subsequent bath application of CGP55845 reversibly reduced the magnitude of the membrane response to baclofen. *B*, summary histogram illustrating the pharmacological profile of GABA$_B$ receptor-mediated responses evoked in SPNs. The peak membrane potential responses (filled columns) and changes in neuronal input resistance (open columns) induced by GABA$_B$ receptor agonists and the effects of antagonists on agonist-induced responses are shown. Error bars represent s.e.m. Numbers above individual bars indicate number of cells tested (*n*). (*$P < 0.01$, **$P < 0.005$, ***$P < 0.03$.)

The effects of GABA$_A$ receptor antagonists on agonist-induced responses

Application of bicuculline (10 μM, $n = 8$) or SR95531 (10 μM, $n = 4$) induced a significant, reversible reduction in the membrane responses induced by muscimol (Fig. 4Aa–c). Bicuculline application reduced the peak amplitude of muscimol-induced membrane hyperpolarization by $61.7 \pm 9.6\%$ from 6.0 ± 0.6 mV to 2.3 ± 1.4 mV in the presence of bicuculline ($P < 0.01$, Fig. 4B). A $70.4 \pm 11.2\%$ ($P < 0.001$) reduction in the associated input resistance change induced by muscimol was also observed in the presence of bicuculline. Likewise, application of SR95531 reduced the muscimol-induced membrane hyperpolarization by $60.3 \pm 6.7\%$, from 8.8 ± 0.9 mV to 3.5 ± 1.2 mV ($P < 0.01$, Fig. 4B), accompanied by a $53.5 \pm 8.9\%$ ($P < 0.03$) reduction in the peak input resistance change induced by muscimol.

The effects of GABA$_B$ receptor antagonists on agonist-induced responses

Application of 2-OH-saclofen (20 μM, $n = 3$) or CGP55845 (200 nM, $n = 5$) suppressed membrane responses induced by baclofen (Fig. 5Aa and b). Application of 2-OH-saclofen reversibly reduced the amplitude of membrane hyperpolarization induced by baclofen by $73.1 \pm 3.5\%$, from 10.1 ± 1.1 mV to 2.3 ± 0.3 mV in the presence of this antagonist ($P > 0.01$, Fig. 5B). A concurrent $45.5 \pm 4.4\%$ ($P < 0.03$) reduction in the peak amplitude of baclofen-induced changes in input resistance was also observed. Bath application of CGP55845 reduced the peak amplitude of baclofen-induced hyperpolarization by $86.2 \pm 8.4\%$ from 9.8 ± 2.7 mV to 1.8 ± 1.0 mV ($P < 0.005$, Fig. 5B), with a corresponding $62.3 \pm 11.1\%$ reduction in the peak change in input resistance induced by baclofen.

Ionic mechanism underlying GABA$_A$ and GABA$_B$ receptor agonist-induced hyperpolarization

Similar to evoked IPSPs, with progressive membrane hyperpolarization from rest, the muscimol induced response decreased in amplitude and reversed to a depolarization (Fig. 6Aa) at a membrane potential of -52 ± 9 mV ($n = 4$, Fig. 6Ab). Current–voltage relationships plotted for four cells, in control conditions and at the peak of the muscimol-induced hyperpolarization (Fig. 6Ba) revealed a reversal potential of -58 ± 4 mV for the muscimol-induced response, again close to the reversal potential for chloride ions under our recording conditions ($n = 4$, Fig. 6Bb). In voltage clamp at a holding potential of -50 mV, application of baclofen (50 μM, 30 s, $n = 5$) induced a sustained

outward current, with a mean peak amplitude of 52.6 ± 6.5 pA. Voltage ramps from −120 to −60 mV at a rate of 10 mV·s⁻¹ were applied in control conditions and at the peak of the baclofen-induced response to investigate the reversal potential of the baclofen-induced current (Fig. 6*Ca*). Baclofen-induced outward currents had a mean reversal potential of −95 ± 3.6 mV ($n = 5$), close to the K⁺ reversal potential under our recording conditions (Fig. 6*Cb*)

Integration of GABAergic inputs by an intrinsic active conductance

When held at membrane potentials close to threshold for firing, in the presence of NBQX (5 μM), D-

APV (10 μM), and idazoxan (200 nM) to block any concurrent glutamatergic and noradrenergic synaptic activity, stimulation of the iLF (Fig. 7*Aa*, $n = 6$) or cLF (Fig. 7*Ab*, $n = 4$) elicited an IPSP which gave rise to rebound firing at the termination of the IPSP. This phenomenon was also observed in some SPNs in response to spontaneous IPSPs (Fig. 7*Ac*, $n = 2$ cells). Brief high-frequency stimulation (10–100 Hz) of the iLF or cLF in SPNs under these recording conditions evoked trains of IPSPs which preceded a rebound excitation and bursts of suprathreshold activity ($n = 4$, Fig. 7*Ad*). The rebound excitation and the resulting action potential firing were insensitive to strychnine (2 μM), but were completely and reversibly abolished
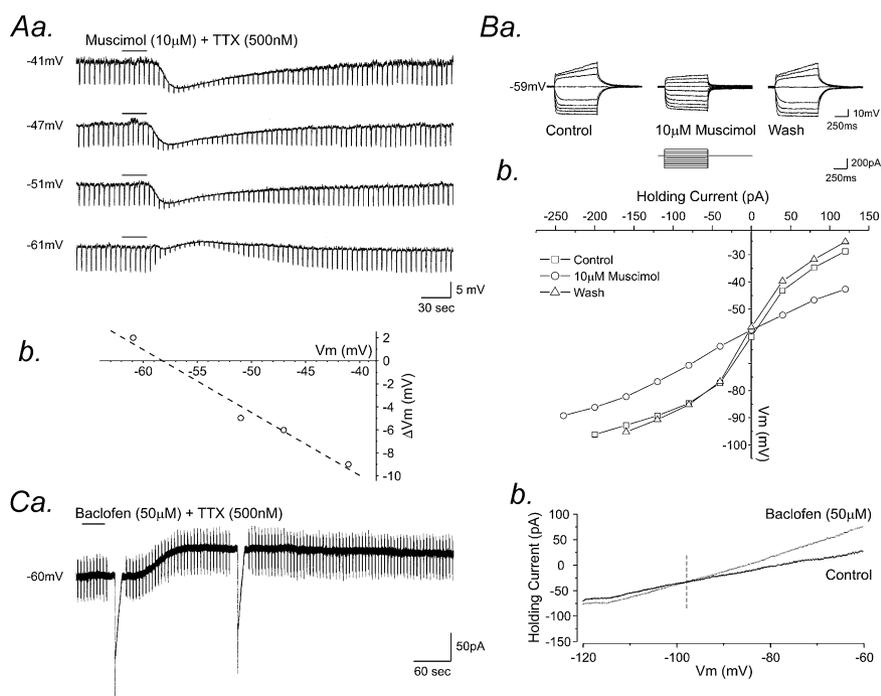

Figure 6. Ionic mechanism underlying GABA_A and GABA_B receptor-mediated inhibition in SPN
Aa, samples of a continuous whole-cell current-clamp record showing muscimol-induced hyperpolarization. The response was associated with a decrease in neuronal input resistance, indicated by the fall in amplitude of electrotonic potentials (downward deflections of the records) evoked in response to hyperpolarizing rectangular wave current pulses (not shown). Progressive membrane hyperpolarization reduced the amplitude of the peak response to muscimol, the response reversing polarity at membrane potentials more negative than −55 mV. The neurone was held at the membrane potentials indicated by the passage of constant negative current via the electrode. *Ab*, plot of the peak amplitude of the muscimol induced response shown in *Aa* against change in membrane potential, showing the response reverses polarity around −58 mV. *Ba*, superimposed samples of a continuous whole-cell current-clamp recording showing membrane potential responses of an SPN to a series of depolarizing and hyperpolarizing rectangular-wave current pulses before, during and after application of muscimol. All responses were obtained in the presence of TTX. *Bb*, plot of the current–voltage (*I–V*) relationships shown in *B*. Note the decrease in the slope of the *I–V* relationship in the presence of muscimol indicating a reduction in neuronal input resistance, and the reversal potential close to that for chloride ions under our recording conditions. *Ca*, whole-cell voltage clamp recording showing application of baclofen produced a sustained outward current. Large downward deflections represent current responses to voltage ramps from −120 to −60 mV (10 mV s⁻¹), shown on a faster time base, superimposed in *Cb*. Note the reversal potential for the baclofen-induced current close to the K⁺ reversal potential under our recording conditions.

by the subsequent application of bicuculline (10 μM, Fig. 7*B*).

We next investigated if voltage-dependent conductances intrinsic to SPNs contributed to this rebound excitation. Injection of small, hyperpolarizing (−10 to −20 pA) rectangular-wave current pulses, to mimic hyperpolarization induced by IPSPs, evoked a time-dependent inward rectification and rebound excitation at the termination of the response to current injection in SPNs in both transverse and longitudinal spinal cord slices ($n = 11$, Fig. 7*C*).

The nature of this time-dependent inward rectification was investigated further in a series of current–voltage relationships generated close to threshold (Fig. 8*A*). The rectification manifests as a slowly developing depolarizing 'sag' when hyperpolarizing current pulses generate membrane responses of around −5 to −10 mV (indicated by arrow in Fig. 8*A*). Application of ZD7288 (10 μM, $n = 3$), a proposed selective blocker of the hyperpolarization-activated cation current I_h (Harris & Constanti, 1995), was without significant effect on the magnitude of the rectification. However, bath application of Cs+ (1 mM,
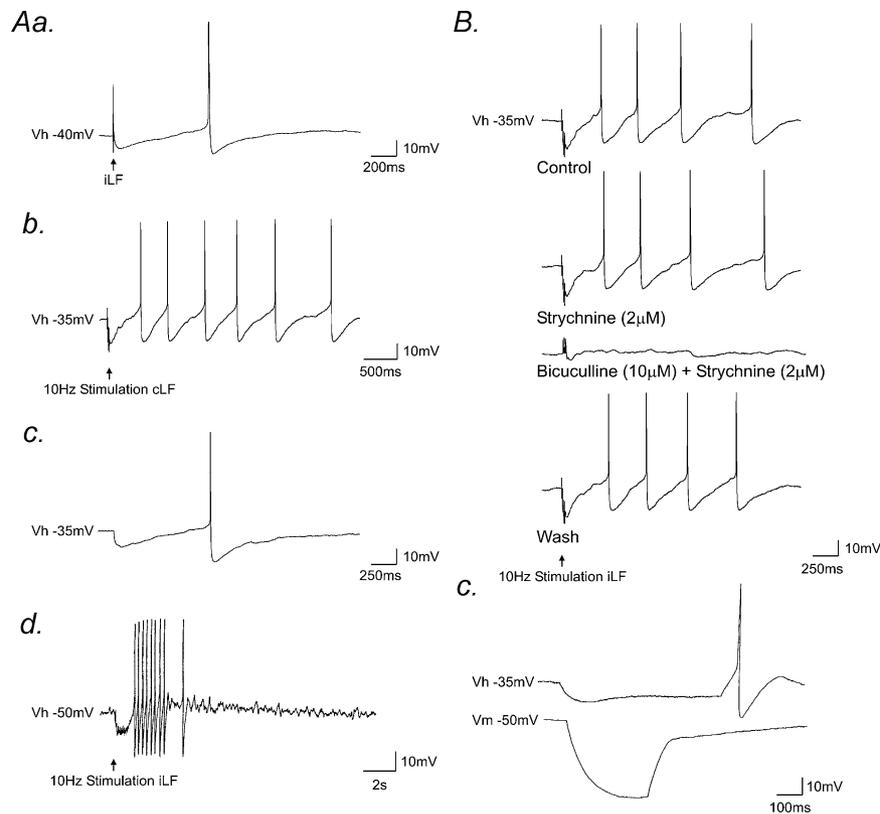
Figure 7. Integration of GABAergic IPSPs by a time-dependent inward rectifying conductance in SPN

Aa, whole-cell current-clamp recordings from an SPN, held close to threshold for firing (V_h − 40 mV), showing stimulation of the iLF elicited an IPSP that gave rise to rebound action potential firing. *Ab*, in the same neurone, repetitive high-frequency stimulation of the cLF evoked fIPSPs which summated, followed by a rebound excitation and a burst of action potentials. *Ac*, recordings from another SPN showing a spontaneous IPSP which gave rise to rebound action potential firing. *Ad*, high frequency stimulation of the iLF elicited fIPSPs that similarly gave rise to a burst of rebound action potential firing. *B*, samples of a continuous whole-cell current clamp recording showing repetitive high frequency (10 Hz) stimulation of the iLF, evoked fast IPSPs which summated, followed by a rebound excitation and action potential firing. The IPSP, rebound excitation and associated action potential firing were all insensitive to strychnine, but were completely and reversibly blocked following subsequent application of bicuculline. *C*, samples of a continuous whole-cell current-clamp recording showing membrane responses to injection of rectangular-wave hyperpolarizing current pulses at holding potentials of −35 mV (top) and −50 mV (bottom). At the resting level of the cell (−50 mV), the SPN was characterized by a transient outward rectification observed as a delayed return to rest of the membrane response to hyperpolarization. At membrane potentials close to threshold (V_{hold} − 35 mV), a marked decrease in neuronal input resistance was apparent and a time-dependent inward rectification and rebound excitation at the termination of the response revealed.

A.

B.

C.
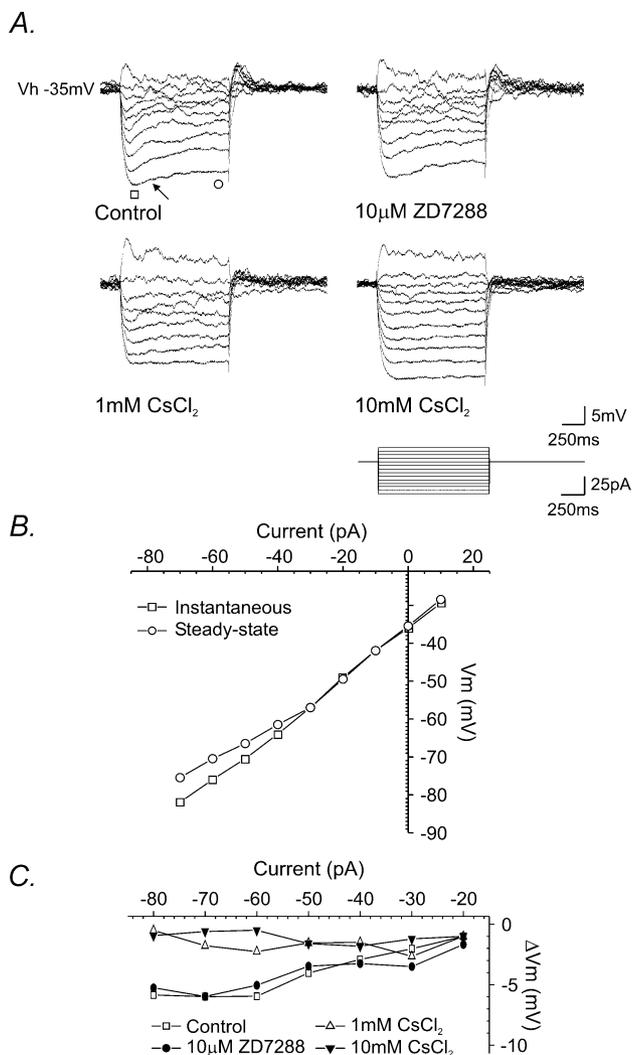
Figure 8. Properties of a time-dependent inward rectifying conductance expressed by SPNs

A, superimposed samples of a continuous whole-cell current-clamp recording showing membrane potential responses of an SPN, held at a membrane potential close to threshold, to a series of depolarizing and hyperpolarizing rectangular-wave current pulses in the presence of TTX. Membrane responses to hyperpolarization were characterized by a time-dependent inward rectification, expressed as a slowly developing depolarizing 'sag' at the peak of the response (indicated by arrow). The rectification was relatively insensitive to ZD7288, partially suppressed in the presence of 1 mM and completely blocked by 10 mM Cs^+. *B*, plot of the current-voltage (*I–V*) relationship for the control trace shown in *A*. Note the decrease in the slope associated with the steady-state response (○) indicating a decrease in input resistance, consistent with opening of ion channels. *C*, plot of the difference between the steady-state and instantaneous membrane responses to current injection showing ZD7288 (●) had little effect on the inward rectification whereas 1 mM $CsCl_2$ (△) and 10 mM $CsCl_2$ (▽), significantly reduced the time-dependent inward rectification compared to control (□).

$n = 5$) partially reduced the rectification and subsequently higher concentrations of Cs^+ (10 mM, $n = 4$) completely and reversibly blocked the rectification (Fig. 8*A* and *C*).

Discussion

In this study, we have utilized whole-cell patch clamp recording techniques to investigate both the role of GABA in synaptic transmission to SPNs and the intrinsic mechanisms by which SPNs integrate these inputs. A major finding of this study is that SPNs receive GABAergic synaptic inputs which project via the lateral funiculi on both sides of the spinal cord. These bilateral GABAergic monosynaptic inputs are mediated via $GABA_A$ receptors. SPNs express both $GABA_A$ receptors, coupled to a chloride conductance, and $GABA_B$ receptors, coupled to a potassium conductance. We found little evidence supporting a role for $GABA_C$ receptors, although our data do not eliminate the possibility of subsets of SPNs utilizing these receptors. Interestingly, we show that activation of GABA-mediated IPSPs in SPNs close to threshold evokes rebound excitations and burst firing. The mechanism underlying this rebound excitation involves a voltage-sensitive active conductance intrinsic to SPNs, characterized by time-dependent inward rectification, activated as a consequence of GABA-mediated synaptic inputs, sensitive to extracellular Cs^+ and reminiscent of I_h described in other neurones. These data suggest GABA may have a role other than as a purely inhibitory neurotransmitter in SPNs. We speculate that a mechanism involving integration of GABAergic bilateral inputs by SPNs and generation of rebound excitation by engaging intrinsic voltage-dependent conductances may be a mechanism by which SPNs can be entrained to physiologically relevant autonomic rhythms.

Origins of GABA-mediated synaptic inputs

Pharmacological blockade of fast EPSPs revealed fast IPSPs in the majority of SPNs following stimulation of the iLF or cLF, through which descending inputs to SPNs pass. This was observed in both transverse and longitudinal spinal cord slices. IPSPs exhibited a consistent latency, rise time and waveform and no failures in response to repetitive stimulation, indicating that these connections were monosynaptic in origin. The fact that cLF stimulation resulted in IPSPs of monosynaptic origin suggests that pathways originating in the contralateral spinal cord were activated rather than polysynaptic interneuronal circuits within the cord.

The origins of these GABAergic inputs to SPNs are difficult to reconcile in the slice preparation. GABA-mediated IPSPs reported in this study were evoked by stimulation of the iLF and cLF, including SPNs in longitudinal slices, stimulated up to five to six segments away from the recording site. Furthermore, we did not observe any evidence of activation of polysynaptic pathways. These data suggest that the fibres activated are most likely bilateral descending inputs from higher centres and/or intraspinal pathways originating in the lateral funiculi (Jansen & Loewy, 1997). Numerous studies have provided evidence that SPNs receive GABAergic synapses from both supraspinal and intraspinal sources (see Llewellyn-Smith, 2002). A known source of supraspinal GABAergic inputs directly innervating SPNs is the rostral ventrolateral medulla (RVLM; Matsumoto *et al.* 1994; Miura *et al.* 1994; Llewellyn-Smith *et al.* 1995; Deuchars *et al.* 1997; Stornetta & Guyenet, 1999). Other supraspinal GABAergic neurones which have been shown to functionally or anatomically impinge on SPNs include the gigantocellular depressor area (GiDA) (Aicher *et al.* 1995; Stornetta & Guyenet, 1999), the rostral ventromedial medulla (parapyramidal area), aspects of the raphe magnus (Loewy, 1981; Millhorn *et al.* 1987; Sasek *et al.* 1990) and the nucleus of the solitary tract (NTS; Blessing *et al.* 1981; Blessing, 1990; Mtui *et al.* 1993; Lewis & Coote, 1995; Stornetta & Guyenet, 1999). All of these areas have been indicated to project to SPN and use GABA as a neurotransmitter.

Sites of contact of GABA synapses.

Monosynaptic GABA-mediated inputs to SPNs evoked by stimulation of the iLF were relatively fast, and comparable to EPSPs evoked from the same site (Spanswick *et al.* 1998). The fast rise time is thus consistent with the site of contact being relatively close to the recording site at the soma. Stimulation of the cLF evoked IPSPs with similar but significantly slower rise times suggesting a site of contact at a site relatively distal to those from the iLF, but closer than those evoked by segmental stimulation (see Spanswick *et al.* 1998). Thus the most likely sites of contact of inputs from both the iLF and cLF are at proximal dendrites or the soma itself. Supporting this notion are spinal transection studies. Descending inputs from these neurones and other higher centres to SPNs descend through the lateral funiculi, from where they branch at right angles towards the IML and SPNs (Anderson *et al.* 1989; Fuxe *et al.* 1990). Several days after a complete spinal transection, over 50% of axosomatic GABAergic boutons are lost from SPNs while axodendritic inputs

decrease by less than 20% (Llewellyn-Smith & Weaver, 2001). Taken together these data strongly suggest bilateral descending GABAergic inputs to SPNs synapse proximal to the soma. The fact that descending glutamatergic inputs similarly synapse bilaterally, proximal to the soma (Spanswick *et al.* 1998), suggests a common topographical and functional organization of fast descending inputs to SPNs.

Mechanisms underlying GABA-mediated bilateral synaptic inputs

IPSPs evoked by stimulation of the iLF or cLF were sensitive to bicuculline, generally insensitive to strychnine and reversed polarity close to the reversal potential for chloride ions under our recording conditions. Similarly, IPSPs were mimicked by bath application of GABA and muscimol in the presence of TTX, responses that were also reversibly inhibited by the GABA$_A$ receptor antagonists bicuculline and SR95531. Exogenous GABA- and muscimol-induced responses also had reversal potentials indicating chloride selectivity. These data, taken together with the observations that agonists for GABA$_C$ receptors were without significant effect on SPN, suggest IPSPs described in this study were mediated by GABA$_A$ receptors coupled to a chloride conductance.

It is worthy of note that in a few cells the IPSP was blocked by a combination of strychnine and bicuculline. Despite the prevailing concept that GABA and glycine are two distinct inhibitory transmitter systems, immunocytochemical and ultrastructural studies have demonstrated coexistence of the two amino acids in terminal boutons of some spinal interneurones and colocalization of GABA, glycine, GABA$_A$ and strychnine-sensitive glycine receptors at the same synapse (Ornung *et al.* 1994; Todd *et al.* 1996; Lévi *et al.* 1999). Also, a common transporter packages these two inhibitory amino acids into synaptic vesicles (Burger *et al.* 1991; Chaudhry *et al.* 1998). Therefore, it has been proposed that GABA and glycine may be released as cotransmitters on postsynaptic targets (Todd *et al.* 1996). These observations together with the fact that functional studies have shown corelease of the two neurotransmitters from spinal cord interneurones, probably from the same synaptic vesicles (Jonas *et al.* 1998; O'Brien & Berger, 1999), raises the possibility that GABA and glycine may be coreleased at certain synapses. Whether bicuculline- and strychnine-sensitive IPSPs described in our study are due to the release of GABA and glycine from the same terminal or from different terminals converging onto the same SPN remains to be clarified.

SPNs express GABA_B receptors

The selective GABA_B receptor agonist baclofen also induced membrane hyperpolarization that was sensitive to the GABA_B receptor antagonists 2-hydroxy-saclofen and CGP55845 confirming the presence of postsynaptic GABA_B receptors in the majority of SPNs. The reversal potential of baclofen-induced responses was close to the reversal potential for K$^+$ ions under our recording conditions, consistent with activation of a potassium-selective conductance. A clear presynaptic role for GABA_B receptors has been demonstrated for both SPNs and other central neurones (Dutar & Nicoll, 1988; Bogan *et al.* 1989; Wu & Dun, 1992; Inokuchi *et al.* 1992). However, the data described in the present study, to our knowledge, are the first to demonstrate expression of postsynaptic GABA_B receptors in SPNs. Despite, the presence of these receptors, indicated by the sensitivity of SPNs to GABA_B receptor agonists and antagonists, we were unable to identify a postsynaptic involvement of these receptors in synaptic transmission from either of the lateral funiculi. There are several explanations that may account for our ability to synaptically activate postsynaptic GABA_A receptors independent of the GABA_B receptors reported here. Firstly, GABA_B receptors may be associated with pathways other than those carried by the lateral funiculi, although a presynaptic role for these receptors here has been suggested previously (Wu & Dun, 1992). As already discussed, GABA-expressing interneurones impinge on SPNs. We were unlikely to have recruited these in our study and have not specifically investigated these pathways. However, a presynaptic role for GABA_B receptors has also been suggested for inputs evoked by stimulation of the dorsal horn and dorsal roots, presumably involving local spinal circuits and segmental interneurones (Wu & Dun, 1992). Alternatively, GABA_B receptors may be localized at extra-synaptic sites and only recruited during prolonged, repetitive stimulation and 'spill-over' of GABA into extrasynaptic domains. Such a mechanism is thought to occur at cerebellar (Hamann *et al.* 2002) and hippocampal (Scanziani, 2000) synapses. However, during the course of our study, repetitive stimulation did not reveal any obvious contribution from GABA_B receptors. Further studies are required to clarify the functional role of postsynaptic GABA_B receptors in SPNs.

*I*_h-like time dependent inward rectification

GABA has to date been primarily considered a purely inhibitory transmitter in SPNs, acting to suppress activity (see Coote, 1988). However, thus far, no studies have taken into account how intrinsic membrane properties of SPNs integrate these inputs. Here we have shown that at membrane potentials close to threshold, both spontaneous and evoked IPSPs gave rise to rebound action potential firing and repetitive high frequency (10 Hz) stimulation evoked trains of fIPSPs which summated, followed by a rebound excitation and bursts of action potential firing. These data suggest SPNs have the intrinsic mechanisms to generate auto-rhythmic activity entrained to GABA-mediated synaptic inputs. A current view is that sympathetic rhythmic discharges emerge principally from networks of supraspinal neurones residing within the brainstem (see Barman & Gebber, 2000). This receives support from data that show correlations between brain-stem activity and peripherally recorded sympathetic rhythms. Several rhythms within the sympathetic nerve firing patterns have been described including a 0.4–1.2 Hz rhythm referred to as the T-rhythm (Johnson & Gilbey, 1996) and both cardiac and respiratory cycle-related rhythms (McAllen & Malpas, 1997; Malpas, 1998; Barman & Gebber, 2000). Both 10 Hz and 2–6 Hz rhythms have been documented in brainstem nuclei with a number of brainstem sites being suggested as origins of these rhythms, including nuclei containing neurones that use GABA as a neurotransmitter (Barman & Gebber, 1997, 2000). Thus, supraspinal activity may be entrained via a GABA-dependent synaptic mechanism and voltage-dependent conductances expressed by SPNs.

A number of mechanisms have been suggested for the generation of auto-rythmicity in SPNs, including both the presence of low voltage-activated T-type conductances (Wilson *et al.* 2002), revealed by activation of adrenoceptors (Yoshimura *et al.* 1987*b*) and by networks of electrotonically coupled SPNs (Logan *et al.* 1996). In the present study, we demonstrate a conductance characterized by time-dependent inward rectification observed at membrane potentials close to threshold, activated by hyperpolarization induced by GABAergic IPSPs and mimicked by injection of hyperpolarizing current pulse injection sufficient to drive the membrane potential more negative than around 5–10 mV below threshold. This conductance is reminiscent of the hyperpolarization-activated time-dependent inward rectification (*I*_h) reported previously in a subpopulation of SPNs in guinea-pig (Inokuchi *et al.* 1993).

*I*_h currents are activated by hyperpolarization and have been described in many other neurones and in cardiac myocytes where they are involved in generating pacemaker activity (see Pape, 1996; Luthi & McCormick, 1998; Robinson & Siegelbaum, 2003). The voltage dependence, ion selectivity and kinetics of *I*_h vary extensively depending

on cell-type and thus the properties of I_h are likely to be tailored to its function within the neurone and the circuits in which it resides (Luthi & McCormick, 1998). In relation to this, the I_h-like conductance described here in SPNs differs from those previously reported for other cells in its relative insensitivity to low concentrations of Cs^+ and ZD7288, possibly reflecting differences in subunit composition related to SPN-specific functions. Key roles for I_h are the regulation of the response to hyperpolarization resulting from IPSPs and a contribution to pacemaker potentials and rhythm generation (Pape, 1996; McCormick & Bal, 1997; Robinson & Siegelbaum, 2003), for example in thalamocortical relay neurones (McCormick & Bal, 1997) and neurones in the inferior olive (Bal & McCormick, 1997).

In SPN, the I_h-like conductance is a non-inactivating non-selective cation conductance activated at membrane potentials between -50 to -70 mV, with a reversal potential around -30 mV reflecting its permeability to both Na^+ and K^+ ions. As I_h is activated by hyperpolarization and depolarizes cells towards its reversal potential, it is capable of mediating rebound excitation from periods of inhibition and thus a key property for rhythm generation.

Conclusion

Our results suggest that SPNs receive monosynaptic, bilateral GABAergic inputs, most likely from supraspinal pathways that synapse proximal to the soma to activate postsynaptic GABA$_A$ receptors coupled to a chloride conductance. Synaptic activation of a rebound excitation mediated by a time-dependent inward rectification expressed intrinsically by SPNs may provide a novel mechanism enabling SPNs to be entrained to rhythms driven from the brainstem or higher centres.

References

Aicher SA, Reis DJ, Nicolae R & Milner TA (1995). Monosynaptic projections from the medullary gigantocellular reticular formation to sympathetic preganglionic neurons in the thoracic spinal cord. *J Comp Neurol* **363**, 563–580.

Anderson CR, McLachlan EM & Srb-Christie O (1989). Distribution of sympathetic preganglionic neurons and monoaminergic nerve terminals in the spinal cord of the rat. *J Comp Neurol* **283**, 269–284.

Backmann SB & Henry JL (1983). Effects of GABA and glycine on sympathetic preganglionic neurons in the upper thoracic intermediolateral nucleus of the cat. *Brain Res* **277**, 365–369.

Bacon SJ & Smith AD (1988). Preganglionic sympathetic neurons innervating the rat adrenal medulla: immunocytochemical evidence of synaptic input from nerve terminals containing substance P, GABA or 5-hydroxytryptamine. *J Autonom Nerv Sys* **24**, 97–122.

Bal T & McCormick DA (1997). Synchronized oscillations in the inferior olive are controlled by the hyperpolarization-activated cation current I_h. *J Neurophysiol* **77**, 3145–3156.

Barman SM & Gebber GL (1997). Subgroups of rostral ventrolateral medullary and caudal medullary raphe neurons based on patterns of relationship to sympathetic nerve discharge and axonal projections. *J Neurophysiol* **77**, 65–75.

Barman SM & Gebber GL (2000). 'Rapid' rhythmic discharges of sympathetic nerves: sources, mechanisms of generation, and physiological relevance. *J Biol Rhythm* **15**, 365–379.

Blessing WW (1990). Distribution of glutamate decarboxylase-containing neurons in rabbit medulla oblongata with attention to intramedullary and spinal projections. *Neurosci* **37**, 171–185.

Blessing WW, Goodchild AK, Dampney RA & Chalmers JP (1981). Cell groups in the lower brain stem of the rabbit projecting to the spinal cord, with special reference to catecholamine-containing neurons. *Brain Res* **221**, 35–55.

Bogan N, Mennone A & Cabot JB (1989). Light microscope and ultrastructural localisation of GABA-like immunoreactive input to retrogradely labelled sympathetic preganglionic neurons. *Brain Res* **505**, 257–270.

Burger PM, Hell J, Mehl E, Krasel C, Lottspeich F & Jahn R (1991). GABA and glycine in synaptic vesicles: storage and transport characteristics. *Neuron* **7**, 287–293.

Cabot JB, Bushnell A, Alessi V & Mendell NR (1995). Postsynaptic gephyrin immunoreactivity exhibits a nearly one-to-one correspondence with gamma-aminobutyric acid-like immunogold-labelled synaptic inputs to sympathetic preganglionic neurons. *J Comp Neurol* **356**, 418–432.

Chaudhry FA, Reimer RJ, Bellocchio EE, Danbolt NC, Osen KK, Edwards RH & Storm-Mathisen J (1998). The vesicular GABA transporter, VGAT, localizes to synaptic vesicles in sets of glycinergic as well as GABAergic neurons. *J Neurosci* **18**, 9733–9750.

Chiba T & Semba R (1991). Immuno-electronmicroscopic studies on the gamma-aminobutyric acid and glycine receptor in the intermediolateral nucleus of the thoracic spinal cord of rats and guinea pigs. *J Autonom Nerv Sys* **36**, 173–182.

Coote JH (1988). The organisation of cardiovascular neurons in the spinal cord. *Rev Physiol Bioch P* **110**, 148–285.

Deuchars SA, Spyner KM & Gilbey MP (1997). Stimulation within the rostral ventrolateral medulla can evoke monosynaptic GABAergic IPSPs in sympathetic preganglionic neurons in vitro. *J Neurophysiol* **77**, 229–235.

Dun NJ, Karczmar AG, Wu SY & Shen E (1993). Putative transmitter systems of mammalian sympathetic preganglionic neurons. *Acta Neurobiol Exp (Warsz)* **53**, 53–63.

Dutar P & Nicoll RA (1988). A physiological role for GABA$_B$ receptors in the central nervous system. *Nature* **332**, 156–158.

Fuxe K, Tinner B, Bjelke B, Agnati LF, Verhofstad A, Steinbusch HG, Goldstein M, Hersh L & Kalia M (1990). Monoaminergic and peptidergic innervation of the intermedio-lateral horn of the spinal cord. *Eur J Neurosci* **2**, 451–460.

Hamann M, Rossi DJ & Attwell D (2002). Tonic and spillover inhibition of granule cells control information flow through cerebellar cortex. *Neuron* **33**, 625–633.

Harris NC & Constanti A (1995). Mechanism of block by ZD 7288 of the hyperpolarization-activated inward rectifying current in guinea pig substantia nigra neurons in vitro. *J Neurophysiol* **74**, 2366–2378.

Inokuchi H, Masuko S, Chiba T, Yoshimura M, Polosa C & Nishi S (1993). Membrane properties and dendritic arborization of the intermediolateral nucleus neurons in the guinea-pig thoracic spinal cord *in vitro. J Autonom Nerv Sys* **43**, 97–106.

Inokuchi H, Yoshimura M, Trzebski A, Polosa C & Nishi S (1992). Fast inhibitory postsynaptic potentials and responses to inhibitory amino acids of sympathetic preganglionic neurons in the adult cat. *J Autonom Nerv Sys* **41**, 53–60.

Jansen ASP & Loewy AD (1997). Neurons lying in the white matter of the upper cervical spinal cord project to the intermediolateral cell column. *Neurosci* **77**, 889–898.

Johnson CD & Gilbey MP (1996). On the dominant rhythm in the discharges of single postganglionic sympathetic neurones innervating the rat tail artery. *J Physiol* **497**, 241–259.

Jonas P, Bischofberger J & Sandkühler J (1998). Co-release of two fast neurotransmitters at a central synapse. *Science* **281**, 419–424.

Krupp J & Feltz P (1993). Synaptic and agonist-induced currents in neonatal rat sympathetic preganglionic neurons in vitro. *J Physiol* **471**, 729–748.

Lévi S, Chesnoy-Marchais Da, Sieghart W & Triller A (1999). Synaptic control of glycine and GABA$_A$ receptors and gephyrin expression in cultured motoneurons. *J Neurosci* **19**, 7434–7449.

Lewis DI & Coote JH (1995). Chemical mediators of spinal inhibition of rat sympathetic neurones on stimulation in the nucleus tractus solitarii. *J Physiol* **486**, 483–494.

Llewellyn-Smith IJ (2002). GABA in the control of sympathetic preganglionic neurons. *Clin Exp Pharmacol P* **29**, 507–513.

Llewellyn-Smith IJ, Arnolda LF, Pilowsky PM, Chalmers JP & Minson JB (1998). GABA- and glutamate-immunoreactive synapses on sympathetic preganglionic neurons projecting to the superior cervical ganglion. *J Autonom Nerv Sys* **71**, 96–110.

Llewellyn-Smith IJ, Cassam AK, Krenz NR, Krassioukov AV & Weaver LC (1997). Glutamate- and GABA-immunoreactive synapses on sympathetic preganglionic neurons caudal to a spinal cord transection in rats. *Neurosci* **80**, 1225–1235.

Llewellyn-Smith IJ, Minson JB, Pilowsky PM, Arnold LF & Chalmers JP (1995). The one hundred percent hypothesis: Glutamate or GABA in synapses on sympathetic preganglionic neurones. *Clin Exp Hypertens* **17**, 323–333.

Llewellyn-Smith IJ & Weaver LC (2001). Changes in synaptic inputs to sympathetic preganglionic neurons after spinal cord injury. *J Comp Neurol* **435**, 226–240.

Loewy AD (1981). Raphe pallidus and raphe obscurus projections to the intermediolateral cell column in the rat. *Brain Res* **222**, 129–133.

Logan SD, Pickering AE, Gibson IC, Nolan MF & Spanswick D (1996). Electrotonic coupling between rat sympathetic preganglionic neurones in vitro. *J Physiol* **495**, 491–502.

Luthi A & McCormick DA (1998). H-current: properties of a neuronal and network pacemaker. *Neuron* **21**, 9–12.

Malpas SC (1998). The rythmicity of sympathetic nerve activity. *Prog Neurobiol* **56**, 65–96.

Matsumoto M, Takayama K & Miura M (1994). Distribution of glutamate- and GABA-immunoreactive neurons projecting to the vasomotor centre of the intermediolateral nucleus of the lower thoracic cord of Wistar rats: a double-labeling study. *Neurosci Lett* **174**, 165–168.

McAllen RM & Malpas SC (1997). Sympathetic activity: characteristics and significance. *Clin Exp Pharmacol P* **24**, 791–799.

McCormick DA & Bal T(1997). Sleep and arousal: thalamocortical mechanisms. *Ann Rev Neurosci* **20**, 185–215.

Millhorn DE, Hokfelt T, Seroogy K, Oertel W, Verhofstad AA & Wu JY (1987). Immunohistochemical evidence for colocalization of gamma-aminobutyric acid and serotonin in neurons of the ventral medulla oblongata projecting to the spinal cord. *Brain Res* **410**, 179–185.

Miura M, Takayama K & Okada J (1994). Distribution of glutamate- and GABA-immunoreactive neurons projecting to the cardioacceleratory centre of the intermediolateral nucleus of the thoracic cord of SHR and WKY rats – a double labelling study. *Brain Res* **638**, 139–150.

Mtui EP, Anwar M, Gomez R, Reis DJ & Ruggiero DA (1993). Projections from the nucleus tractus solitarii to the spinal cord. *J Comp Neurol* **337**, 231–252.

O'Brien JA & Berger AJ (1999). Cotransmission of GABA and glycine to brain stem motoneurons. *J Neurophysiol* **82**, 1638–1641.

Ornung G, Shupliakov O, Otterson OP, Storm-Mathisen J & Cullheim S (1994). Immunohistochemical evidence for co-existence of glycine and GABA in nerve terminals of cat spinal motorneurones: an ultrastructural study. *Neuroreport* **5**, 889–892.

Pape HC (1996). Queer current and pacemaker: the hyperpolarization-activated cation current in neurons. *Ann Rev Physiol* **58**, 299–327.

Robinson RB & Siegelbaum SA (2003). Hyperpolarization-activated cation currents: From molecules to physiological function. *Ann Rev Physiol* **65**, 453–480.

Sasek CA, Wessendorf MW & Helke CJ (1990). Evidence for co-existence of thyrotropin-releasing hormone, substance P and serotonin in ventral medullary neurons that project to the intermediolateral cell column in the rat. *Neurosci* **35**, 105–119.

Scanziani M (2000). GABA spillover activates postsynaptic GABA$_B$ receptors to control rhythmic hippocampal activity. *Neuron* **25**, 673–681.

Spanswick D, Renaud LP & Logan SD (1998). Bilaterally evoked monosynaptic EPSPs, NMDA receptors and potentiation in rat sympathetic preganglionic neurones in vitro. *J Physiol* **509**, 195–209.

Stornetta R & Guyenet PG (1999). Distribution of glutamic acid decarboxylase mRNA-containing neurons in rat medulla projecting to thoracic spinal cord in relation to monoaminergic brainstem neurons. *J Comp Neurol* **407**, 367–380.

Todd AJ, Watt C, Spike RC & Sieghart W (1996). Colocalization of GABA, glycine, and their receptors at synapses in the rat spinal cord. *J Neurosci* **16**, 974–982.

Whyment AD, Van den Top M & Spanswick D (2000). GABA$_A$ and GABA$_B$ receptor-mediated inhibition of rat sympathetic preganglionic neurones in vitro. *J Physiol* **528.P**, 118*P*.

Wilson JMM, Coderre E, Renaud LP & Spanswick D (2002). Active and passive membrane properties of rat sympathetic preganglionic neurones innervating the adrenal medulla. *J Physiol* **545**, 945–960.

Wilson JMM & Spanswick D (1998). Bilateral GABA-mediated synaptic inputs to rat sympathetic preganglionic neurones in a longitudinal spinal cord slice. *J Physiol* **506.P**, 154*P*.

Wu SY & Dun NJ (1992). Presynaptic GABA$_B$ receptor activation attenuates synaptic transmission to rat sympathetic preganglionic neurons in vitro. *Brain Res* **572**, 94–102.

Yoshimura M, Polosa C & Nishi S (1987*a*). Slow IPSP and the noradrenaline-induced inhibition of the cat sympathetic preganglionic neurone *in vitro. Brain Res* **419**, 383–386.

Yoshimura M, Polosa C & Nishi S (1987*b*). Noradrenaline induces rhythmic bursting in sympathetic preganglionic neurons. *Brain Res* **420**, 147–151.

Acknowledgements